

Nanoscale

Accepted Manuscript



This is an *Accepted Manuscript*, which has been through the Royal Society of Chemistry peer review process and has been accepted for publication.

Accepted Manuscripts are published online shortly after acceptance, before technical editing, formatting and proof reading. Using this free service, authors can make their results available to the community, in citable form, before we publish the edited article. We will replace this *Accepted Manuscript* with the edited and formatted *Advance Article* as soon as it is available.

You can find more information about *Accepted Manuscripts* in the [Information for Authors](#).

Please note that technical editing may introduce minor changes to the text and/or graphics, which may alter content. The journal's standard [Terms & Conditions](#) and the [Ethical guidelines](#) still apply. In no event shall the Royal Society of Chemistry be held responsible for any errors or omissions in this *Accepted Manuscript* or any consequences arising from the use of any information it contains.

SCHOLARONE™
Manuscripts

Nanoscale Accepted Manuscript

Cite this: DOI: 10.1039/c0xx00000x

www.rsc.org/xxxxxx

Full papers

Dextran-coated superparamagnetic nanoparticles as potential cancer drug carriers *in vivo*

Mingli Peng,^{a,b} Houli Li,^b Zhiyi Luo,^b Jian Kong,^c Yinsheng Wan,^d Leming Zheng,^{*c} Qinlu Zhang,^b Hongxin Niu,^e Alphons Vermorken,^b Wim Van de Ven,^f Chao Chen,^b Xikun Zhang,^e Fuqiang Li,^b Lili Guo^b and Yali Cui^{*b}

Received (in XXX, XXX) Xth XXXXXXXXX 20XX, Accepted Xth XXXXXXXXX 20XX

DOI: 10.1039/b000000x

Dextran-coated superparamagnetic iron oxide nanoparticles (DSPIONs) have gained considerable interest, because of their biocompatibility and biosafety in clinics. Doxorubicin (Dox), a widely used chemotherapeutic drug, always has limited applications in clinical therapy due to its serious side effects of dose-limiting irreversible cardiotoxicity and myelo suppression. Herein, DSPIONs were synthesized and developed as magnetic carriers for doxorubicin. The Dox-DSPIONs conjugates were evaluated in *in vitro* test of Dox release, which showed pH-dependence with the highest release percentage of 50.3% at pH 5.0 and lowest release percentage of 11.8% in physiological environment. The cytotoxicity of DSPIONs and Dox-DSPIONs evaluated by MTT assay indicated that DSPIONs had no cytotoxicity and the conjugates had significantly reduced the toxicity ($IC_{50}=1.36 \mu\text{g mL}^{-1}$) compared to free Dox ($IC_{50}=0.533 \mu\text{g mL}^{-1}$). Furthermore, confocal microscopic data of cell uptake suggest that the less cytotoxicity of Dox-DSPIONs may be attributed by the cellular internalization of the conjugates and sustainable release of DOX from the formulation in the cytoplasm. More importantly, the results from rabbit VX2 liver tumor model test under the external magnetic field showed that the conjugates had approximately twice anti-tumor activity and two and half folds of animal survival rate, respectively, compared to free Dox. Collectively, our data have demonstrated that Dox-DSPIONs have the less toxicity with better antitumor effectiveness in *in vitro* and *in vivo* application, suggesting that the conjugates have potentials to be developed into chemo-therapeutic formulations.

Introduction

Recently, nanomedicine for the delivery of anticancer drugs to tumors has gained considerable interest. It offers a possible way to target drug-delivery to tumor site and to concentrate the cytotoxicity on tumor cells. Ideally, anticancer nanomedicines should: (i) be safe with nontoxic carriers; (ii) have a high drug-loading efficiency; (iii) cause an improved therapeutic response; (iv) lead to a decrease of undesirable toxicity on normal cells; (v) be easy to prepare.⁴⁻⁶

Among all drug carriers, hybrid magnetic nanoparticles, especially superparamagnetic iron oxide nanoparticles (SPIONs), have attracted significant attention due to their unique characteristics,⁷⁻¹³ including a fast response to an external magnetic field. Also, many biocompatible polymers, such as chitosan, PEG, dextran, PVA and PVP, have been utilized for the development of SPIONs in drug delivery systems.^{7, 11, 14-17}

Dextran, a polysaccharide, has been extensively and successfully used for various *in vivo* applications. Dextran-coated SPIONs provide desirable stability with no reported toxicity. In fact, dextran-coated iron oxide nanoparticles, marketed as Ferridex I.V. and Ferumoxytol, have been recently approved as contrast agents for MRI and iron deficiency anemia.¹⁸⁻²² In addition to these applications, dextran-coated SPIONs (DSPIONs) also provide a powerful nanoparticle platform for the targeted delivery of therapeutics.^{7, 23, 24}

Doxorubicin (Dox), a widely used chemotherapeutic drug, has

already been developed into liposome formulations for clinical application. However, such formulations cause anaphylactic shock in patients with a history of hypersensitivity reactions to the components of liposomes.²⁵ Special attention has also been given to the risk of myocardial damage from cumulative doses of the drug just as other commercial products. Furthermore, the dermal toxicity for the liposomes formulation is shown to be more serious on patients.²⁶ Thus, new formulations with Dox have to be developed.

Given the outstanding characteristics of SPIONs, the popularity of Dox in clinical settings, and yet the unavailability of better Dox formulations, some studies combine the SPION and DOX for the cancer therapy. However, lack of systematic research, commercial availability of SPION and convenient utility of Dox still remains. Targeted nanomedicine of Dox are yet to be developed. Herein, we aimed to develop a magnetically guided drug delivery formula to reduce the toxicity of Dox by adopting the dextran-coated superparamagnetic nanoparticles as drug carriers. Firstly, DSPIONs and Dox-DSPIONs were synthesized and characterized in aqueous solution based on our previous studies of nanoparticles.^{27, 28} Then the cytotoxicity was evaluated by MTT assay *in vitro*, for both DSPIONs and the conjugates of Dox-DSPIONs. The advantages of less toxicity, minimum release in physiological environment and good magnetic behaviour make Dox-DSPIONs ready to be applied in the *in vivo* animal model guided by an external magnetic field. Our experimental data strongly suggest that Dox-DSPIONs could be a novel drug formulation in clinical cancer treatment.

Materials and Methods

Materials

Dextran-40 was purchased from Shanghai Huamao Pharmaceutical Co., Ltd. Iron salts were from Sigma-Aldrich (China) Co., Ltd. NaOH was purchased from Xi'an Fuli Chemical Reagents Co., Ltd. Cell culture media (RPMI 1640) and fetal bovine serum (FBS) were obtained from Gibco Co., Ltd. DMSO was obtained from Sigma-Aldrich (China) Co., Ltd. MTT (3-(4,5-dimethylthiazol-2-yl)-2, 5-diphenyl tetrazolium bromide) was purchased from Amresco Co., Ltd. Dimethylsulphoxide (DMSO) and Doxorubicin (Dox) were purchased from Hisun Co., Ltd., China. Water used in the experiments was de-ionized, and all organic solvents were of analytical reagent grade.

Nanoparticles preparation

15 Preparation of SPIONs

Iron oxide nanoparticles were synthesized by co-precipitation of ferrous and ferric salts with excess NaOH.²⁹ Briefly, 3.48 g ferrous and ferric salts were dissolved in water, and then 1 mol L⁻¹ NaOH was added with vigorous stirring. The reaction was allowed to proceed for 20 min at room temperature, and then the temperature was raised up to 60-65 °C and kept for another 20 min. The formation of iron-oxide nanoparticles was indicated by color change of the solution from yellow to light brown to black. The resultant Fe₃O₄ particles were collected and washed with plenty of water in order to neutralize the pH of the samples. A magnet was used in order to concentrate the particles. Finally, the synthesized Fe₃O₄ particles were re-suspended in water.

Preparation of DSPIONs

2 g of Dextran-40 was added into a 250 mL flask containing 20 mL 0.5 M NaOH solution. After the dextran was dissolved, 400 mg iron oxide magnetic particles were added into the flask. The mixture was ultrasonicated for 5 h below 45 °C to composite and iron oxide nano particles together.³⁰ Then, the black suspension was obtained. The dialysis treatment to remove the excess dextran and inorganic salts was carried out by transferring suspension to dialysis membranes with cutoff of 10 KDa till the particles were brought to neutral pH. Then, DSPIONs were stored at room temperature for further use and characterization.

Preparation of Dox-DSPIONs

The drug loading experiment was carried out as follows: 100 mg of Dox dissolved in water was added into a 100 mL flask containing 1 g of DSPIONs under stirring (180 rpm). The reaction was continued at 37 °C for at least 24 h. The concentration of Dox in solution was monitored with UV-Vis spectrometer at 480 nm. Then, the prepared Dox-loaded dextran-coated SPIOs were stored at 4 °C for further use and characterization.

Characterization of nanoparticles

The size distribution of DSPIONs was assessed by dynamic light scattering (DLS) instrument (Malvern Mastersizer 2000, Malvern Instrument, Worcestershire, UK). The shape and surface morphology was investigated by transmission electron microscope TEM (Hitachi H-600, Hitachi Corporation, Tokyo,

Japan). Further, the particles were analyzed for phase composition using X-ray diffraction (XRD) on a diffractometer (Bruker Smart Apex II CCD; Cu K α radiation, $\lambda = 1.5418 \text{ \AA}$, Bruker AXS Inc., Karlsruhe, Germany). In order to confirm the iron oxide phase, the nature of coating and its bonding on the surface, Fourier transform infrared spectra (FTIR) was recorded between 4000 and 400 cm⁻¹ on a Nicolet 5700 FTIR spectrometer (Thermo Nicolet 5700, Thermo Nicolet Corporation, Wisconsin, USA). Finally, vibrating sample magnetometry (VSM) was used to measure the magnetic properties of SPIONs and DSPIONs with a magnetometer (LakeShore-655, Lake Shore Inc., USA) at room temperature.

In vitro release of Dox from Dox-DSPIONs

The release studies were carried out as follows. Dox-DSPIONs were added into a tube with 15 mL water at pH values of 5.0, 6.0, and 7.0. The mixture was stirred at 180 rpm, at 37 °C. 5 mL of sample solutions were taken for detection at specific time intervals and the same volume of water was supplemented. The release experiment lasted over 7 days. The concentration of Dox was determined by measuring UV-vis absorbance of the solutions at 480 nm (Agelient Uv-vis Spectrophotometer).

75 Cell lines and cell culture

Human hepatocellular carcinoma (HepG2) cells and normal cells (LO2) were obtained from the Fourth Military Medical University. LO2 and HepG2 cells were cultured in 100 mL culture flasks using RPMI-1640 medium supplemented with 10% FBS and 1% penicillin, streptomycin (1 \times 10⁴ units mL⁻¹). The cultures were maintained at 37 °C in an atmosphere of 5% CO₂ and 95% relative humidity.

Cytotoxicity assays

MTT assays were carried out to evaluate the potential cytotoxicity of DSPIONs. LO2 and HepG2 cells were seeded into 96 well plates at 200 μ L/well with density of 5 \times 10⁴ cells mL⁻¹ and incubated for 24 h. Then, the medium was removed, and the suspensions of DSPIONs with concentrations ranging from 0 μ g mL⁻¹ to 2000 μ g mL⁻¹ were added to the wells. The cells were incubated at 37 °C for 24 h. 20 μ L of MTT (5 mg mL⁻¹ in PBS pH 7.4) was added to each well. After incubation for 4 h, 150 μ L DMSO was added, and the solution was vigorously mixed and transferred to centrifuge tubes by each well and centrifuged at 13000 rpm for 10 min to eliminate the interference of spectrophotometry readings from the high concentration of DSPIONs.³¹ The supernatant was then transferred to a fresh 96 wells plate. The absorbance of each well was read on an ELx-800 Universal Microplate Reader (BIOTEK Instruments, Vermont, USA) at 570 nm. The relative cell viability (%) related to the control wells containing cell culture medium was calculated by the following Equation:

$$\text{Cell viability (\%)} = (A_{\text{Test sample}} / A_{\text{Control}}) \times 100\%$$

where $A_{\text{Test sample}}$ is the absorbance of the test sample and A_{Control} is the absorbance of the control.

105 Cellular uptake of Dox-DSPIONs

Uptake and intracellular distribution of Dox-DSPIONs nanocomposite were evaluated by confocal laser scanning

microscopy (CLSM, TCS SP5, Leica Microsystems, Germany). HepG2 cells were cultured in dishes with a cover slip at the density of 1×10^5 cell/dish. After 24 h, cells were exposed to $5 \mu\text{g mL}^{-1}$ Dox-DSPIONs nanoparticles and incubated at 37°C . Cells cultured with DMEM medium were used as the control group. At different time points after incubation, cells were washed 3 times with PBS and fixed with a 4% paraformaldehyde solution, and cellular nuclei were stained with 4,6-diamidino-2-phenylindole (DAPI, Sigma, USA). The confocal microscope was equipped with DAPI filters, and images were captured with oil-immersion objectives.

Animals and cell lines

New Zealand white rabbits (weight, 2.0-2.5 kg) selected randomly from Shandong Academy of Agricultural Sciences, were used for *in vivo* anti-tumor activity studies. The Animal Research Committee of the Medical Research Institution approved all experiments and surgical procedures. At first, the animals were acclimatized at a temperature of $25 \pm 2^\circ\text{C}$ and a relative humidity of $70 \pm 5\%$ under natural light/dark conditions for 1 week and were fed with food and water *ad libitum*. Prior to the experiments the animals were kept under fasting overnight. VX2 hepatocarcinoma cells were obtained from the Fourth Military Medical University and were maintained as tumor lines in the laboratory.

Anti-tumor activity of Dox-DSPIONs in a rabbit VX2 hepatoma model

Inoculation of VX2 carcinoma fragment was performed in 50 New Zealand white rabbits. The rabbits were anesthetized and the hairs over the abdominal region of the rabbits were shaved, and the region was then cleaned with saline water. 1-2 mm^3 fragments of VX2 tumor tissues were implanted into the liver. The wound was kept sterile, and antibiotics (80 million IU of penicillin) were injected into the muscles after the implantation. The animals were observed by CT (64-Slice CT, Siemens, Germany). Based on the CT scan results, 36 rabbits with a tumor diameter of 13.15 ± 0.17 mm were randomly divided into 3 groups (each $n=12$) and were given intra-arterial injections of 5% glucose, free Dox (0.5 mg kg^{-1}) and Dox-DSPIONs (0.5 mg kg^{-1}). The Dox-DSPIONs group was then treated with a magnetic field (3,000 GS) for 2h after injection.

An incision was made in the anesthetized rabbits to expose the right femoral artery. A micro-catheter was then inserted into the femoral artery with its tip remaining in the hepatic artery. Digital subtraction angiography (DSA) was used to confirm the location and morphology of the VX2 hepatoma. Then, the preparation was gradually injected into the hepatic artery, with great care taken to avoid an efflux of the preparation out of the artery. After intra-arterial injection, digital subtraction angiography was performed again, followed by removal of the catheter, ligation of the femoral artery, and closure of the operative wound to complete the operative procedure. After the operation, the behavior, appetite and vital signs, especially the rate of respiration were closely monitored in all rabbits. CT examinations were performed on rabbits of 3 groups before surgery and on 10 d and 20 d after surgery and the tumor diameters were measured so as to calculate the tumor growth ratio. 8 weeks after surgery, the rabbits were sacrificed and hepatic tumors were collected for pathological

examinations.

Statistical analysis

All values are expressed as the mean \pm SD. The data were analyzed using the Student's *t* test or the ANOVA test. A *P* value of <0.05 was considered statistically significant. GraphPad Prism (GraphPad Software Inc., San Diego, California, USA) was used for these analyses.

Results and discussion

Physicochemical properties of DSPIONs

To initiate this study, first, we synthesized DSPIONs. The size of DSPIONs was then characterized by TEM and DLS (Fig. 1A and 1B). The data showed that the diameter of DSPIONs was about 10 nm, which is in accordance with the size of iron oxide particles obtained by co-precipitation methods as previously described.²⁹ The hydrodynamic diameter of DSPIONs was 168.6 ± 27.8 nm with desirable size distribution and stability in suspension, while the diameter of the commercial SPIO MRI contrast agent Ferridex I.V was between 80 and 150 nm with the average size of 112 nm.²² The diameter of DSPIONs is larger than the commercial particles but still in the appropriate range for a drug carrier notably between 100-200 nm.⁹

To further characterize DSPIONs, the components of DSPIONs were analyzed by FT-IR. The spectra for Fe_3O_4 , dextran and DSPIONs were shown in Fig. 1C. The characteristic absorption bands of the magnetite at 583 cm^{-1} are attributed to Fe-O bond (Fig. 1C-a).³² The typical stretching of O-H, C-O-C at $3600\text{-}3200 \text{ cm}^{-1}$ and $1150\text{-}1085 \text{ cm}^{-1}$ of dextran-40 were evident (Fig. 1C-b). The spectrum of DSPIONs showed both absorptions of magnetite at 588 cm^{-1} and dextran at $1150\text{-}1085 \text{ cm}^{-1}$ exhibiting the contents of dextran-40 and Fe_3O_4 nanoparticles (Fig. 1C-c). The contents of magnetite and dextran in DSPIONs magnetic particles as determined by ICP-AAS and the anthrone colorimetric method, are 28% and 72%, respectively (Fig. 1D).³³ The X-ray diffraction pattern of the DSPIONs is shown in Fig. 1E-b. All of the characteristic peaks in the pattern can be easily indexed for Fe_3O_4 (220), (311), (422), (511) and (440) (JCPDS card No. 85-1436), suggesting that DSPIONs keep the crystal structure of magnetite (Fig. 1E-a) and that the preparation process does not affect the crystalline structure of Fe_3O_4 .³⁴

The magnetic behavior of obtained particles was investigated by VSM. All particles showed superparamagnetic properties at room temperature (Fig. 1F, Fe_3O_4 (a), DSPIONs (b)). Fe_3O_4 nanoparticles gave a saturated magnetization of 61.2 emu g^{-1} , while DSPIONs showed a value of 15.2 emu g^{-1} at room temperature. The decrease of the saturated magnetization could be ascribed to the magnetite fraction decrease to 28% in DSPIONs particles.³⁵ This is in accordance with the results of ICP-AAS of DSPIONs. The fast response to the external magnetic field, the stable composition and the desirable stability of DSPIONs in solution make the particles ideal nanocarriers.

Both the commercial dextran coated SPIO MRI contrast agent Ferridex I.V. and DSPIONs are comparable with regard to the composition of the nanoparticles with dextran and superparamagnetic iron oxide. However, the differences are i) the core sizes of SPIOs and ii) the size distribution and iii) the surface charges. The Ferridex I.V. nanoparticles contain SPIOs

that are approximately 5 nm in diameter and are embedded in a meshwork of linear dextran, while DSPIONs have the core size of about 10 nm. The twice-larger core size of SPIONs with high crystallinity in DSPIONs would lead to a better response in an external magnetic field, which suggest that the nanoparticles could be guided magnetically during the drug delivery.³⁶ The hydrodiameter of DSPIONs is larger, but they are still in the appropriate range for a drug carrier of 100-200 nm.^{9, 22} and they

have a more negative surface charge (-16.2 ± 0.7 mV) than the commercial particles (-13 mV). The more negative surface charge would absorb more of the positively charged anticancer drugs such as doxorubicin hydrochloride and cisplatin. Thus, the fast response to an external magnetic field, the stable composition and the appropriate size distribution and more negative surface charge of DSPIONs in solution make this system a good candidate for being an ideal nanocarrier for doxorubicin.

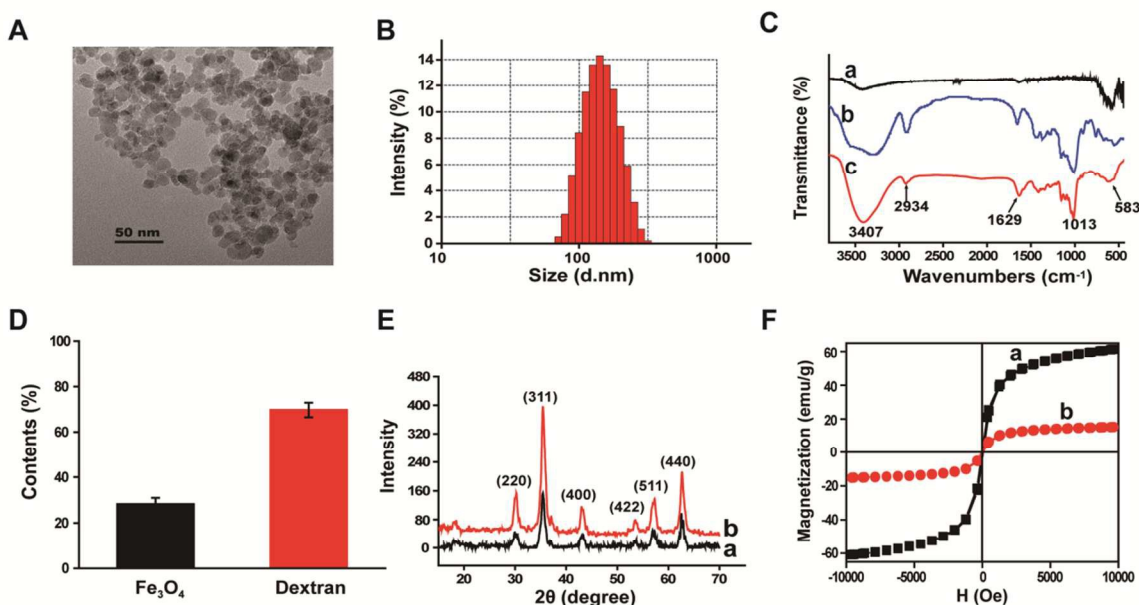


Fig. 1 The characterization of Dextran-coated superparamagnetic iron oxide nanoparticles (DSPIONs); A: TEM image of DSPIONs (scale bar, 50 nm); B: The size distribution of DSPIONs in water measured by dynamic light scattering. C: FTIR spectrum of Fe₃O₄ (a), Dextran (b) and DSPIONs (c); D: The mass percentage of Fe₃O₄ and Dextran in DSPIONs; E: X-ray diffraction pattern of Fe₃O₄ (a) and DSPIONs (b); F: Magnetization curves of Fe₃O₄ (a) and DSPIONs (b).

Physicochemical properties of Dox-DSPIONs

In order to synthesize and characterize Dox-DSPIONs, firstly, the Dox and DSPIONs were mixed with a mass ratio of 1:10 and incubated for 6 h to form Dox-DSPIONs conjugates. The capacity of DSPIONs nanoparticles for Dox was $98.3 \mu\text{g mg}^{-1}$ with high loading efficiency (Fig. 2A). The hydrodynamic diameter of Dox-DSPIONs (266.7 ± 49.0 nm) was larger than that of unloaded DSPIONs (Fig. 2B) and the zeta potential of Dox-DSPIONs turned into a positive charge (21.3 ± 3.8 mV, Fig. 2C-b), while before Dox was loaded, DSPIONs nanoparticles were negatively charged (-16.2 ± 0.7 mV, Fig. 2C-a) due to the dextran coating.^{22, 37} Dox loading onto DSPIONs largely depends on the chemical and physical properties of the nanoparticles surfaces and coating. In our case, the desirable loading is likely due to the following reasons, a) by adsorption on the magnetic core of SPIONs, where the iron cation on the iron oxide particle surface can promote the deprotonation of the phenolic groups and form a complex to the particle surface, b) by diffusion in the coating materials of dextran, and c) by electrostatic interaction between particles and Dox. Dox is positively charged at pH 7.4, and can be adsorbed onto the particles surface, stabilized by negatively charged dextran.¹⁵

Next, the drug release from Dox-DSPIONs conjugates was

studied. *In vitro* assays were performed at pH values of 5.0, 6.0, and 7.0 to simulate the lysosomal, the endosomal and the extracellular matrix components of the tumor cellular microenvironment, respectively. As shown in Fig. 2D, the amount of Dox released into a simulated physiological environment (pH 7.0) was relatively low, with only 11.8% of Dox being released within 120 h. These findings suggest that the release of Dox under neutral conditions such as blood plasma and normal liver tissue would be minimum, thereby reducing the systemic distribution of Dox during drug delivery. However, the Dox release rate from Dox-DSPIONs into the medium simulating the acidic tumor extracellular pH (pH 5.0) was significantly higher (50.3%). This increase in Dox release may be due to the degradation of dextran at acidic pH buffer solution. These results further suggest that the Dox release rate from Dox-DSPIONs is pH-dependent. This drug release behavior has been observed in Dox-nanomedicine of PEGylated nanoparticles³⁸ and glycyrrhetic acid-modified alginate nanoparticles.²³

Cytotoxicity assays and cellular uptake of Dox-DSPIONs

To evaluate the cytotoxicity of DSPIONs or Dox-DSPIONs, the MTT assay was used in LO2 and HepG2 cells. The results showed that DSPIONs ($50\text{-}2000 \mu\text{g mL}^{-1}$) had no obvious cytotoxicity on LO2 (Fig. 3A) and HepG2 cells (Fig. 3B). Dox-

DSPIONs show the inhibited ability of HepG2 cells as well as the free Dox. However, the IC_{50} values of Dox-DSPIONs were $1.36 \mu\text{g mL}^{-1}$ are 2.5 times larger than that of free Dox ($0.533 \mu\text{g mL}^{-1}$), indicating that the Dox-DSPIONs have significantly reduced the cytotoxicity of Dox (Fig. 3C).

We then investigated the mechanism involved in the above process by cell culture and confocal microscopy. The data showed that only small amounts of Dox were observed in the cells within 3 hours of treatment. 12 hours later, Dox was detectable in the cytoplasm but not in the nuclei (Fig. 3D). While in the case of free Dox, the fluorescence was clearly observed both

in the cytoplasm and the nuclei within 3 hours. The results suggest that Dox is released from Dox-DSPIONs after the nanocomposite penetrates into the cytoplasm. With incubation time increasing from 24 to 48 hours, a large amount of fluorescence of Dox was visible in the cytoplasm and in the nuclei of the Dox-DSPIONs treated cells. This result suggests that Dox is released from conjugates with high efficiency after being taken up by the cells. The cellular internalization of Dox-DSPIONs likely occurs via endocytosis

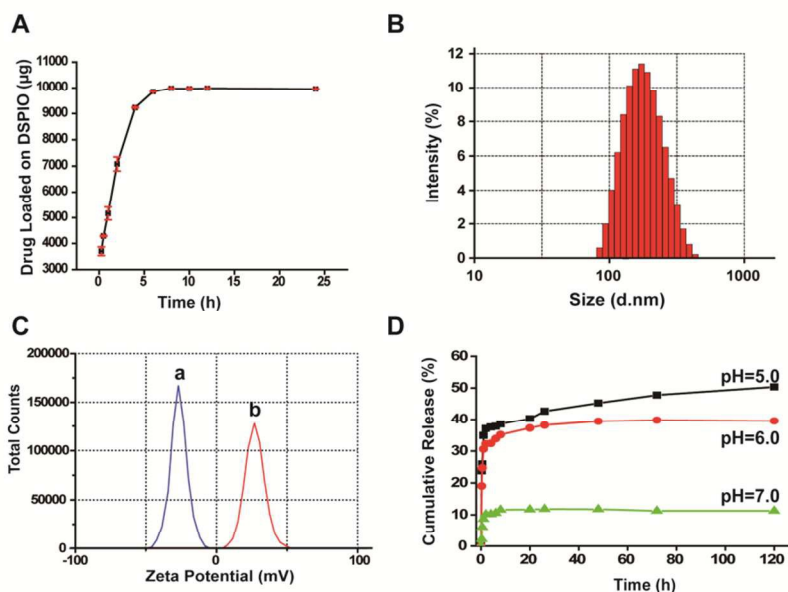


Fig. 2 The characterization of Dox-DSPIONs; A: Kinetic adsorption of Dox on the DSPIONs, B: The size distribution of Dox-loaded DSPIONs in water measured by DLS; C: The zeta potential of DSPIONs(a) and Dox-loaded DSPIONs (b); D: The kinetics release of Doxorubicin from the DSPIONs at different pH value.

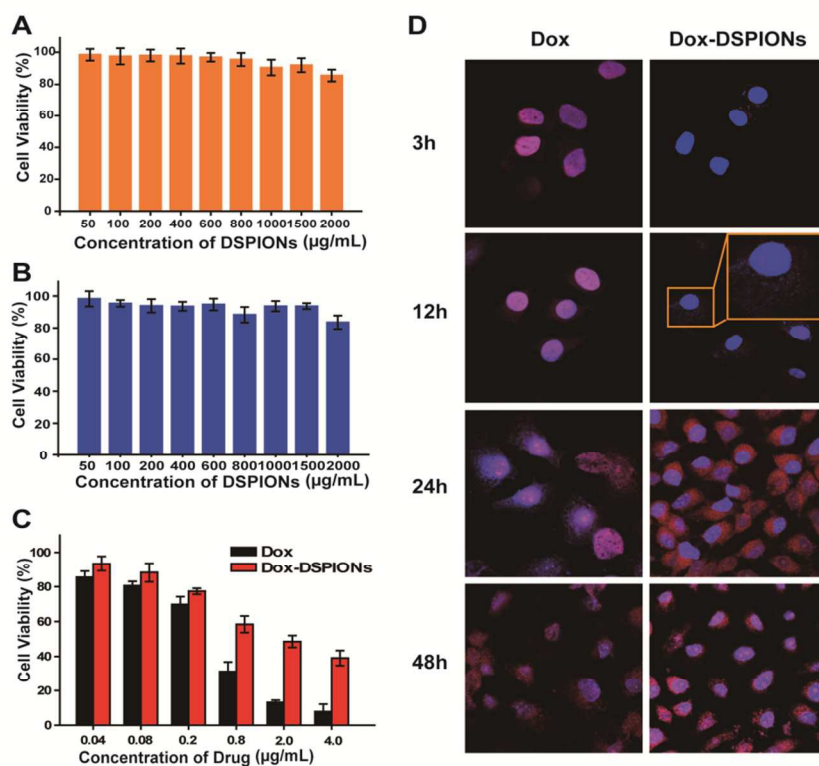


Fig. 3 Cytotoxicity evaluation of DSPIONs by MTT assay with 24 h incubations with different cell lines (A: Normal human liver cells LO2, B: Human hepatocellular carcinoma cells HepG2); the cytotoxicity evaluation of free Dox and Dox-DSPIONs with HepG2 cells (C); and confocal laser scanning fluorescent microscopy image (D) of HepG2 cells incubated with free Dox ($1 \mu\text{g mL}^{-1}$) and Dox-DSPIONs ($1 \mu\text{g mL}^{-1}$) for 3, 12, 24 h. Red fluorescence is from Dox and blue fluorescence is from the DAPI. In contrast to free Dox, the fluorescence of the Dox in the conjugate is only detected when they are released.

and the conjugates may be enzymatically degraded in the acidic environment of lysosomes.¹⁸ Subsequently, Dox is released from DSPIONs nanocarriers in the cytoplasm and enters into the nuclei. Those released Dox molecules thereafter permeate through the intracellular milieu, eventually reaching and penetrating the cell nuclei where they intercalate between DNA base pairs.³⁹ This unique mechanism will contribute greatly to the maintenance of the concentration of the drug in the tumor cells.

Anti-tumor activity of Dox-DSPIONs *in vivo*

Based on the low *in vitro* cytotoxic activity of Dox-DSPIONs against hepatic carcinoma cells, the anti-tumor activity in the VX2 hepatoma model *in vivo* was also evaluated. The anti-tumor

model was established as previously described.^{40, 41} Under CT evaluation, the arterial catheterization process was successfully performed and the external magnet was fixed on the tumor position as shown in Fig. 4A. It was observed that the Dox-DSPIONs were injected into the catheter and most of them rapid moved to location with magnetic field during the administration. We also found no significant differences in the original tumor diameter among the groups of control, free Dox and Dox-DSPIONs before the injection ($P > 0.05$). As shown in Fig. 4B, ten days after surgery, the average tumor diameter was significantly smaller in Dox-DSPIONs group than in the other

Cite this: DOI: 10.1039/c0xx00000x

www.rsc.org/xxxxxx

Full papers

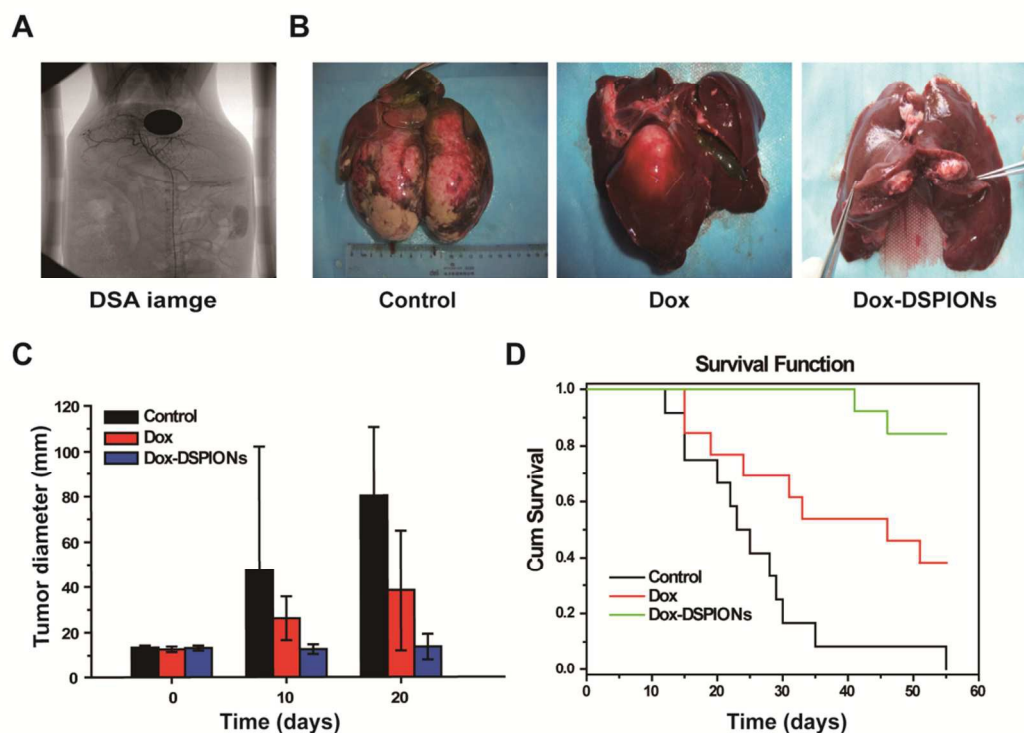


Fig. 4 The *in vivo* antitumor effects in the rabbit VX2 liver tumor model. Rabbits were implanted fragments of VX2 tumor tissues into the liver. When the tumor diameter reached ca. 1.3 cm, rabbits were given intra-arterial injections of 5% glucose injection, free Dox (0.5 mg kg⁻¹) and Dox-DSPIONs (0.5 mg kg⁻¹). The Dox-DSPIONs group was then treated with a magnetic field (3,000 GS) for 2h after injection. A: the photographs of DSA image and the tumors; B: the tumor diameter of the three groups at 0, 10, 20 days; C: the photographs of the tumors; D: the survival curves of three groups.

two groups. 20 days after surgery, tumors treated with 5% glucose injection and free Dox showed continuous growth with similar tendency at a relatively high rate. The average tumor diameter in these groups reached 80.2 mm and 31.5 mm, in accordance with the tumor growth rate which was 595% and 302%, respectively. For the Dox-DSPIONs group, the average tumor diameter and tumor growth rate was 13.7 mm and 104%, which indicates that the tumors grew steadily with a lower rate than the other two groups. This result strongly suggests that free Dox and Dox-DSPIONs can inhibit the growth of tumor, but Dox-DSPIONs have a much better efficacy (Fig. 4B). The tumors from the three groups were also observed by macroscopic examination. The tumors showed invasive growth and no discernable normal lobular architecture (Fig. 4C). None of the rabbits died of complications related to the implantation, the arterial catheterization, or the drug injection process during this experiment. The animal survival rate 55 days after surgery in the Dox-DSPIONs group was 83.3%, much higher than that in 5% glucose injection group (0%) and free Dox group (33.3%), which further signify that free Dox and Dox-DSPIONs can effectively prolong the survival period in the rabbit VX2 transplanted tumor

model, and Dox-DSPIONs have a better efficacy (Fig. 4C). The superior anti-tumor effect of Dox-DSPIONs might be attributed to the less leak of Dox to normal tissues, magnetically guided delivery of the drug to the tumor site and the sustained release of Dox after efficient cellular uptake in the tumor tissue.^{42, 43}

Conclusion

In conclusion, our data have clearly demonstrated that Dox-DSPIONs have potential as a novel delivery system for Dox in anticancer therapy. In this conjugate, SPIONs and dextran act as core nanoparticles for efficient drug loading. The complexes between DSPIONs and Dox are high efficiency with pH-dependent drug release. The conjugate acts as a new Dox drug magnetic delivery platform, with much lower systemic toxicity both *in vitro* and *in vivo*. Dox-DSPIONs present a desirable anti-tumor efficacy superior to free Dox in rabbit animal model. We thus contend that Dox-DSPIONs could be developed into a novel formulation for use in clinical treatment of cancer in the future.

Acknowledgements

This work was supported by Key National Science and Technology Projects on “Key New Drug Creation and Manufacturing” (Grant No. 2012ZX09506001001), “973” National S&T Major Project (Grant No. 2011CB503900), National Science Foundation of Shaanxi Province (Grant No. 2012JM2003, 2012JQ4026) and National Natural Science Foundation of China (Grant No. 21303136, 1170101 and 81370235).

Notes and references

^a Key Laboratory of Synthetic and Natural Functional Molecular Chemistry of Ministry of Education, College of Chemistry and Materials Science, Northwest University, Xi'an, 710069, P. R. China. Fax: +86-29-88303551; Tel: +86-29-88302333; E-mail: mlpeng@nwu.edu.cn

^b National Engineering Research Center for Miniaturized Detection Systems, College of Life Sciences, Northwest University, Xi'an, 710069, P. R. China. Fax: +86-29-88303551; Tel: +86-29-88302383; E-mail: yalicuti@nwu.edu.cn

^c The Institute of Cardiovascular Sciences and Institute of Systems Biomedicine, School of Basic Medical Sciences, and Key Laboratory of Molecular Cardiovascular Sciences of Ministry of Education, Peking University Health Science Center, Beijing, 100191, P. R. China. Fax: +86-10-82802769; Tel: +86-10-82805452; E-mail: zhengl@bjmu.edu.cn

^d Department of Biology, Providence College, Providence, RI 02918, USA.

^e Department of Minimally Invasive Surgery, Affiliated Hospital of Shandong Academy of Medical Science, Jinan, 250031, P. R. China

^f Laboratory for Molecular Oncology, Department of Human Genetics, University of Leuven, Belgium

1. P. Boyle and B. Lebin, *World Health Organization Press*, 2008.
2. D. A. Gewirtz, M. L. Bristol and J. C. Yalowich, *Current opinion in investigational drugs*, 2010, **11**, 612-614.
3. D. R. Friend and S. Pangburn, *Medicinal research reviews*, 1987, **7**, 53-106.
4. A. Maksimenko, F. Dosio, J. Mougin, A. Ferrero, S. Wack, L. H. Reddy, A. A. Weyn, E. Lepeltier, C. Bourgaux, B. Stella, L. Cattel and P. Couvreur, *Proceedings of the National Academy of Sciences of the United States of America*, 2014, **111**, E217-226.
5. R. Duncan, *Nature reviews. Cancer*, 2006, **6**, 688-701.
6. Y. Matsumura and H. Maeda, *Cancer research*, 1986, **46**, 6387-6392.
7. U. O. Hafeli, *International journal of pharmaceuticals*, 2004, **277**, 19-24.
8. A. K. Gupta and M. Gupta, *Biomaterials*, 2005, **26**, 3995-4021.
9. U. Jeong, T. Herricks, E. Shahar and Y. Xia, *Journal of the American Chemical Society*, 2005, **127**, 1098-1099.
10. H. C. Huang, S. Barua, G. Sharma, S. K. Dey and K. Rege, *Journal of controlled release : official journal of the Controlled Release Society*, 2011, **155**, 344-357.
11. Y. Chen, H. Chen, S. Zhang, F. Chen, L. Zhang, J. Zhang, M. Zhu, H. Wu, L. Guo, J. Feng and J. Shi, *Advanced Functional Materials*, 2011, **21**, 270-278.
12. K. Li, D. Ding, D. Huo, K.-Y. Pu, N. N. P. Thao, Y. Hu, Z. Li and B. Liu, *Advanced Functional Materials*, 2012, **22**, 3107-3115.
13. T. Sundstrom, I. Daphu, I. Wendelbo, E. Hodneland, A. Lundervold, H. Immervoll, K. O. Skafnesmo, M. Babic, P. Jendelova, E. Sykova, M. Lund-Johansen, R. Bjerkvig and F. Thorsen, *Cancer research*, 2013, **73**, 2445-2456.
14. L. Ao, B. Wang, P. Liu, L. Huang, C. Yue, D. Gao, C. Wu and W. Su, *Nanoscale*, 2014, **6**, 10710-10716.
15. J. Gautier, E. Allard-Vannier, E. Munnier, M. Souce and I. Chourpa, *Journal of controlled release : official journal of the Controlled Release Society*, 2013, **169**, 48-61.
16. K. M. Kamruzzaman Selim, Y. S. Ha, S. J. Kim, Y. Chang, T. J. Kim, G. Ho Lee and I. K. Kang, *Biomaterials*, 2007, **28**, 710-716.
17. L. Pan, J. Liu, Q. He and J. Shi, *Advanced materials*, 2014, **26**, 6742-6748.
18. Y. L. Li, L. Zhu, Z. Liu, R. Cheng, F. Meng, J. H. Cui, S. J. Ji and Z. Zhong, *Angewandte Chemie*, 2009, **48**, 9914-9918.
19. Y. Chao, M. Makale, P. P. Karmali, Y. Sharikov, I. Tsigelny, S. Merkulov, S. Kesari, W. Wrasidlo, E. Ruoslahti and D. Simberg, *Bioconjugate chemistry*, 2012, **23**, 1003-1009.
20. J. M. Richards, C. A. Shaw, N. N. Lang, M. C. Williams, S. I. Semple, T. J. MacGillivray, C. Gray, J. H. Crawford, S. R. Alam, A. P. Atkinson, E. K. Forrest, C. Bienek, N. L. Mills, A. Burdess, K. Dhaliwal, A. J. Simpson, W. A. Wallace, A. T. Hill, P. H. Roddie, G. McKillop, T. A. Connolly, G. Z. Feuerstein, G. R. Barclay, M. L. Turner and D. E. Newby, *Circulation. Cardiovascular imaging*, 2012, **5**, 509-517.
21. P. A. Hals, P. C. Sontum, E. Holtz, J. Klaveness and P. Rongved, *Current drug delivery*, 2013, **10**, 134-143.
22. C. Tassa, S. Y. Shaw and R. Weissleder, *Acc. Chem. Res.*, 2011, **44**, 842-852.
23. C. Zhang, W. Wang, T. Liu, Y. Wu, H. Guo, P. Wang, Q. Tian, Y. Wang and Z. Yuan, *Biomaterials*, 2012, **33**, 2187-2196.
24. P. K. Working, M. S. Newman, T. Sullivan and J. Yarrington, *The Journal of pharmacology and experimental therapeutics*, 1999, **289**, 1128-1133.
25. J. Szebeni, F. Muggia, A. Gabizon and Y. Barenholz, *Advanced drug delivery reviews*, 2011, **63**, 1020-1030.
26. M. S. Ewer, F. J. Martin, C. Henderson, C. L. Shapiro, R. S. Benjamin and A. A. Gabizon, *Seminars in oncology*, 2004, **31**, 161-181.
27. X. Chao, Z. Zhang, L. Guo, J. Zhu, M. Peng, A. J. Vermorken, W. J. Van de Ven, C. Chen and Y. Cui, *PLoS one*, 2012, **7**, e40388.
28. W. Hui, F. Shi, K. Yan, M. Peng, X. Cheng, Y. Luo, X. Chen, V. A. Roy, Y. Cui and Z. Wang, *Nanoscale*, 2012, **4**, 747-751.
29. C. Yali, H. Wenli, w. Huirong, W. Lijun and C. Chao, *Science in China(Series B Chemistry)*, 2004, **47**, 152-158.
30. Z. Xia, G. Wang, K. Tao and J. Li, *Journal of Magnetism and Magnetic Materials*, 2005, **293**, 182-186.
31. U. O. Hafeli, J. S. Riffle, L. Harris-Shekhawat, A. Carmichael-Baranauskas, F. Mark, J. P. Dailey and D. Bardenstein, *Molecular pharmaceuticals*, 2009, **6**, 1417-1428.
32. C. W. Jung, *Magnetic Resonance Imaging*, 1995, **13**, 675-691.
33. T. S. Jr and E. Melvin, *Analytical chemistry*, 1953, **25**, 1656.
34. H. Deng, X. Li, Q. Peng, X. Wang, J. Chen and Y. Li, *Angewandte Chemie*, 2005, **117**, 2842-2845.
35. A. Prakash, H. Zhu, C. J. Jones, D. N. Benoit, A. Z. Ellsworth, E. L. Bryant and V. L. Colvin, *ACS nano*, 2009, **3**, 2139-2146.
36. C. Hui, C. Shen, T. Yang, L. Bao, J. Tian, H. Ding, C. Li and H.-j. Gao, *J.Phys.Chem.C*, 2008, **112**, 11336-11339.
37. X. Xu, H. Shen, J. Xu, J. Xu, X. Li and X. Xiong, *Applied surface science*, 2005, **252**, 494-500.
38. J. Gautier, E. Munnier, A. Paillard, K. Herve, L. Douziech-Eyrolles, M. Souce, P. Dubois and I. Chourpa, *International journal of pharmaceuticals*, 2012, **423**, 16-25.
39. F. Peng, Y. Su, X. Ji, Y. Zhong, X. Wei and Y. He, *Biomaterials*, 2014, **35**, 5188-5195.
40. B. Zhang, Z. Luo, J. Liu, X. Ding, J. Li and K. Cai, *Journal of Controlled Release*, 2014, **192**, 192-201.
41. C. Huang, Z. Tang, Y. Zhou, X. Zhou, Y. Jin, D. Li, Y. Yang and S. Zhou, *International journal of pharmaceuticals*, 2012, **429**, 113-122.
42. W. Cao, Y. Wan, Z. Liang, Y. Duan, X. Liu, Z. Wang, Y. Liu, J. Zhu, X. Liu and H. Zhang, *European Journal of Radiology*, 2010, **73**, 412-419.
43. S. H. Kim, D. Choi, H. K. Lim, M. J. Kim, K. M. Jang, S. H. Kim, W. J. Lee, J. Lee, Y. H. Jeon and J. H. Lim, *European Journal of Radiology*, 2006, **59**, 413-423.